

ORIGINAL ARTICLE

Implication of proliferation gene biomarkers in pulmonary hypertension

Yi Yan^{1,2}  | Rong Jiang³ | Ping Yuan³  | Li Wen⁴ | Xiao-Bin Pang⁵ | Zhi-Cheng Jing⁶ | Yang-Yang He⁵ | Zhi-Yan Han⁷

¹Institute for Cardiovascular Prevention (IPEK), Ludwig-Maximilians-University Munich, Munich, Germany

²DZHK (German Centre for Cardiovascular Research), partner site Munich Heart Alliance, Munich, Germany

³Department of Cardio-Pulmonary Circulation, Shanghai Pulmonary Hospital, Tongji University School of Medicine, Shanghai, China

⁴Department of Cardiology, The First Affiliated Hospital, Chongqing Medical University, Chongqing, China

⁵School of Pharmacy, Henan University, Henan, China

⁶State Key Laboratory of Complex, Severe, and Rare Diseases, and Department of Cardiology, Peking Union Medical College Hospital, Chinese Academy of Medical Sciences and Peking Union Medical College, Beijing, China

⁷State Key Laboratory of Cardiovascular Disease and FuWai Hospital, Chinese Academy of Medical Sciences and Peking Union Medical College, Beijing, China

Correspondence

Yang-Yang He, School of Pharmacy, Henan University, North Section of Jinming Avenue, Longting District, Kaifeng, Henan Province, China.
Email: hi_heyangyang@163.com

Zhi-Yan Han, State Key Laboratory of Cardiovascular Disease and FuWai Hospital, Chinese Academy of Medical Sciences and Peking Union Medical College, 167 Beilishi Road, Beijing 100037, China.
Email: zhiyanhan2006@hotmail.com

Funding information

This work was supported by National Natural Science Foundation of China (81630003, 82170058), Science Foundation for Outstanding Young Scholars of Henan Province (212300410027), Key Research Project of Ningxia Hui Autonomous Region (2019BFG02027) and Project for College of Traditional Chinese Medicine of Henan University (No. 2021YJYZ07).

Abstract

Objective/Background: Proliferation is a widely recognized trigger for pulmonary hypertension (PH), a life-threatening, progressive disorder of pulmonary blood vessels. This study was aimed to identify some proliferation associated genes/targets for better comprehension of PH pathogenesis.

Methods: Human pulmonary arterial smooth muscle cells (hPASMCs) were cultured in the presence or absence of human recombinant platelet derived growth factor (rhPDGF)-BB. Cells were collected for metabolomics or transcriptomics study. Gene profiling of lungs of PH rats after hypoxia exposure or of PH patients were retrieved from GEO database.

Results: 90 metabolites (VIP score >1, fold change >2 or <0.5 and $p < .05$) and 2701 unique metabolism associated genes (MAGs) were identified in rhPDGF-BB treated hPASMCs compared to control cells. In addition, 1151 differentially expressed genes (313 upregulated and 838 downregulated) were identified in rhPDGF-BB treated hPASMCs compared to control cells (fold change >2 or <0.5 and $p < .05$). 152 differentially expressed MAGs were then determined, out of which 9 hub genes (IL6, CXCL8, CCL2, CXCR4, CCND1, PLAUR, PLAU, HBEGF and F3) were defined as core proliferation associated hub genes in protein protein interaction analysis. In addition, the hub gene-based LASSO model can predict the occurrence of PH (AUC = 0.88).

Yi Yan and Rong Jiang contributed equally and are first authors.

Yang-Yang He and Zhi-Yan Han contributed equally and are last authors.

This is an open access article under the terms of the Creative Commons Attribution License, which permits use, distribution and reproduction in any medium, provided the original work is properly cited.

© 2021 The Authors. *Animal Models and Experimental Medicine* published by John Wiley & Sons Australia, Ltd on behalf of The Chinese Association for Laboratory Animal Sciences.

The expression of CXCR4, as one of the hub genes, was positively correlated to immune cell infiltrates.

Conclusion: Our findings revealed some key proliferation associated genes in PH, which provide the crucial information concerning complex metabolic reprogramming and inflammatory modulation in response to proliferation signals and might offer therapeutic gains for PH.

KEYWORDS

metabolism associated genes, metabolomics, proliferation, pulmonary hypertension, transcriptomics

1 | INTRODUCTION

Pulmonary hypertension (PH) is a vicious cardio-pulmonary disorder and manifested by progressive increase in pulmonary artery pressure and pulmonary vascular resistance, which ultimately leads to right heart failure and even death.¹ Multiple factors including genetic predisposing genes,^{2,3} epigenetic modulations,^{4,5} inflammation,⁶ altered metabolism^{7,8} and environment insults such as hypoxia⁹ are reported to cause the remodeling of the pulmonary vasculature, as manifested by overproliferation, anti-apoptosis and high migratory capability of vascular cells.¹⁰ According to WHO classification, PH is categorized into 5 main groups, with pulmonary arterial hypertension (PAH) to be Group 1 PH.¹¹ As of today, most of therapies are targeted against PAH, including endothelin receptor antagonists, phosphodiesterase type 5 inhibitors, and prostacyclin analogues.¹² These therapies help to improve exercise capacity, hemodynamics and quality of life. However, none of the current treatments are actually curative and long-term prognosis still remains poor.

As proliferation is a critical trigger for PH development, the factors/elements in regulation of proliferation has emerging as a research focus against pulmonary vascular remodeling. For example, low-dose FK506 reverses PH in rats with medial hypertrophy following monocrotaline and neointima formation of Sugen5416/Hypoxia PH rats (a severe PH model) via rescue of bone morphogenetic protein receptor-2 (BMPR2) signaling dysfunction,¹³ which is widely recognized in circulating system and lung tissues of PH patients.^{14,15} At the mechanism level, the induction of BMPR2 signaling by FK506 is not only associated with the reversal of endothelial cells (ECs) dysfunction, but also with the inhibition of pulmonary arterial smooth muscle cells (PASMCs) proliferation, as evident by a direct effect of FK506 in inhibiting platelet derived growth factor (PDGF) induced proliferation. PDGF is regarded as the most potent mitogen for PASMCs¹⁶ and the subtype PDGF-BB (dimeric form of PDGF-B) is widely applied as a stimuli for PASMCs functional study in PH. Moreover, a higher PDGF-B and its receptor PDGFR-beta mRNA expression was observed in small pulmonary arteries from patients with idiopathic PAH, and both PDGF-B and PDGFR-beta were localized in PASMCs in small remodeled pulmonary arteries.¹⁷ The elevated PDGF signaling contributes to the pathobiology of

PAH¹⁸ by regulation of proliferation and migration of pulmonary vascular SMCs, and its inhibition abolishes pulmonary vascular remodeling in two PH models.¹⁹ Therefore, a better understanding into PDGF-BB mediated gene/metabolite profiling would aid in the discovery of novel target to reverse vascular remodeling. Systemic or local inflammation is another feature of PH.^{20,21} The proliferation associated alteration in lung tissues and its impact on immune cell infiltration would also shed some light on the pathogenesis of PH.

Here, we sought to scrutinize the gene/metabolite alterations in PASMCs in response to PDGF-BB, identify some proliferation associated genes/targets by virtue of metabolomics and transcriptomics and unveil the potential link between proliferation and inflammation, which might provide new approaches for the treatment of PH.

2 | METHODS

2.1 | Cell culture and sample collection

Human pulmonary artery smooth muscle cells (hPASMCs) were purchased from the American Type Culture Collection (ATCC; Cat#. PCS-100-023) and cultured at 37°C in the incubator containing 5% CO₂ in Dulbecco's Modified Eagle Medium: Nutrient Mixture F-12 (DMEM/F-12) (Gibco; Cat#. 11320033) containing 10% (v/v) fetal bovine serum (FBS) (Gibco; Cat#.10437-028), 100 µg/ml streptomycin and 100 U/ml penicillin (Gibco; Cat#. 15140-122).

For metabolomic study, hPASMCs were seeded into 6-well plates at a density of 0.5×10^6 /ml. Twenty-four hours later cells were starved with DMEM/F-12 containing 0.5% fetal bovine serum for another 24 h. Cells were gently washed with PBS followed by addition of fresh blank medium with recombinant human PDGF-BB (rhPDGF-BB) (R& D systems; Cat#. 220-BB) at the concentration of 20 ng/ml or vehicle for 24 h ($n = 6$ /group). Cells were collected, washed, centrifuged at 300 g at 4°C for 10 min and resuspended with PBS to reach a final density of 1×10^5 /ml. One milliliter cell suspension per sample was centrifugated at 300 g at 4°C for 5 min. Supernatants were discarded and cell pellets were stored at -80°C. Freezing and thawing cycle was avoided before sample processing in case of potential degradation of metabolites.

For bulk RNA sequencing, hPASCs were seeded into 6-well plates and starved as aforementioned. Cells were gently washed with PBS followed by addition of fresh blank medium with recombinant human PDGF-BB (rhPDGF-BB) (R&D systems; Cat#. 220-BB) at the concentration of 20 ng/ml or vehicle BB for 6 h ($n = 3/\text{group}$) before collection. Cells were then washed, centrifuged at 300 g at 4°C for 10 min. Supernatants were discarded and cell pellets were stored at -80°C before further use.

2.2 | LC/MS analysis and data process

One milliliter of MeOH:ACN:H₂O (2:2:1, v/v) solvent mixture was added into the cell samples followed by sonification. Cells were prepared as previously described.⁷ Liquid chromatographic separation for processed samples was achieved on a ZORBAX Eclipse Plus C18 column (2.1 × 100 mm, 3.5 μm, Agilent, USA) maintained at 45°C, whereas mass spectrometry was performed on a Nexera X2 system (Shimadzu, Japan) coupled with a Triple TOF 5600 quadrupole-time-of-flight mass spectrometer (AB SCIEX, USA). All the steps for LC/MS analysis and data preprocessing were depicted in our previous study.⁷

We used partial least squares discriminant analysis (PLS-DA) to distinguish the overall difference in metabolic profile between rhPDGF-BB treated- and control hPASCs. Variables with a variable weight value (Variable Important in Projection, VIP) >1 were considered to be distinguishing among groups. The enriched metabolic pathways of metabolites with VIP >1 and fold change (FC) >2 or <0.5 and corresponding $p < .05$ between rhPDGF-BB treated- versus vehicle treated hPASCs were further analyzed by Metaboanalyst²² (v5.0, <https://www.metaboanalyst.ca>). The top 10 enriched metabolite pathways were selected as key word for analysis in Genecards²³ (<https://www.genecards.org>). Genes with relevance score >8 were defined as metabolism associated genes (MAGs).

2.3 | RNA isolation, RNA sequencing and analysis

Total mRNA was isolated from frozen hPASCs with Trizol (Invitrogen). RNA libraries were constructed for sequencing on the BGISEQ-500 sequencing platform (BGI, Wuhan, China) with a single-end read length of 50 bp. Briefly, high-quality reads were aligned to the human reference genome (GRCh38) using HISAT2 (version 2.0.4) and Bowtie2 (version 2.2.5). Normalized gene expression was calculated using the fragments per kilobase per million mapped reads (FPKM). Student's *t* test was used for differentially expressed genes (DEGs) analysis. DEGs were defined as fold change (FC) of gene expression >2 or <0.5 and corresponding $p < .05$ between rhPDGF-BB treated- versus vehicle treated hPASCs. Principle component analysis (PCA) was adopted to distinguish the overall difference in expression gene profiling between groups. The enriched pathways of DEGs were identified by functional annotation tool Metascape²⁴

(<https://metascape.org/gp/index.html#/main/step1>) and visualized in bar plot with `barplot` function in R.

2.4 | Identification and validation of hub genes

The intersection of MAGs and DEGs in rhPDGF-BB treated- versus vehicle treated cells was regarded as critical proliferation associated genes. Next, protein-protein interaction of those genes were analyzed by STRING (v11.0, <https://string-db.org>).²⁵ CytoHubba plugin with MCC algorithm or MCODE plugin in Cytoscape (v 3.8.2)²⁶ were used to find the hub genes of the network identified by STRING.

Hub genes were validated in human lungs from the dataset GSE117261²⁷ with 25 control subjects and 58 PH patients and in rat lungs from the dataset GSE85618²⁸ including 4 PH rats after hypoxia exposure and 4 rats in normoxic condition. All the datasets were obtained from Gene Expression Omnibus (GEO) database.

2.5 | Construction of LASSO regression model

Least Absolute Shrinkage and Selection Operator (LASSO) regression model was constructed with the hub gene panel by `glmnet` package in R to distinguish PH patients from control subjects. A model index for each sample was generated using the regression coefficients to weight the expression of each hub gene. Samples of dataset GSE117261 were randomly assigned to training set (70%) and test set (30%). ROC curves were generated to evaluate the ability of LASSO model to identify PH by `ROCR` package.

2.6 | Immune cell infiltrates and its relationship with CXCR4

To decipher the immune cell heterogeneity of human lung tissues, cell type enrichment analysis from gene expression data of GSE117261 for different immune cells was performed based on `webtool xCell`²⁹ (<https://xcell.ucsf.edu>). The relationship of CXCR4 with different cell infiltrates were examined by Pearson correlation analysis. $p < .05$ represents significant correlation.

2.7 | Data visualization and statistics

Volcano plot was generated to display the overview of distinguishing metabolites or genes between rhPDGF-BB treated- and vehicle treated hPASCs. The expression of the distinct metabolites or indicated genes in each individual sample was plotted in heatmap. Hub gene network was visualized by Cytoscape. Correlation of immune cell infiltrates with CXCR4 expression was plotted in scatterplot in R.

Data are presented as the mean ± standard error of the mean (SEM). Statistical differences between two groups were evaluated with 2-tailed unpaired *t* test if the samples were normally distributed. Otherwise,

Mann-Whitney test was used to detect the difference (GraphPad Prism 8). $p < .05$ denotes significant differences between two groups.

3 | RESULTS

3.1 | Altered metabolic signature in hPASMCs in response to rhPDGF-BB and identification of MAGs

As illustrated in flow chart of Figure 1, the metabolite profiles in rhPDGF-BB treated hPASMCs and control hPASMCs were investigated. The hPASMCs in the presence of rhPDGF-BB separated well from control cells according to PLS-DA analysis (Figure 2A) and had a higher proliferation capacity compared to that of control cells (Figure S1). 329 up-regulated and 20 down-regulated metabolites were unveiled in rhPDGF-BB treated hPASMCs compared to that of vehicle treated cells ($FC > 2$ or < 0.5 , $p < .05$) (Figure 2B). Among those changed metabolites, 90 metabolites (87 were upregulated and 3 were downregulated) had a VIP score > 1 and their expressions in each sample were displayed in Figure S2. Expression of distinguishing metabolites including top 40 upregulated and 3 downregulated metabolites with VIP score > 1 were visualized in Figure 2C. Next, 90 metabolites distinguishing rhPDGF-BB treated- and control hPASMCs were enriched in metabolite sets such as phenylalanine, tyrosine and tryptophan biosynthesis, taurine and hypotaurine metabolism, tyrosine metabolism etc., with the top 10 documented

in Figure 2D. The top 10 metabolite sets were then selected for further analysis in GeneCards. According to the results, there were 2701 unique genes identified as MAGs with a relevance score > 8 .

3.2 | Identification of differentially expressed MAGs in response to rhPDGF-BB treatment

To further narrow down the panel of MAGs in response to rhPDGF-BB treatment, we first determined the DEGs in rhPDGF-BB treated hPASMCs compared to control cells. The rhPDGF-BB treated hPASMCs distributed distinctly from control cells according to PCA analysis (Figure 3A). Compared to control cells, there were 313 up-regulated and 838 down-regulated genes displayed in rhPDGF-BB treated hPASMCs in Figure 3B. The Venn diagram showed 152 shared genes between DEGs and MAGs (Figure 3C). Of the 152 differently expressed MAGs, 49 were increased and 103 decreased in hPASMCs after rhPDGF-BB treatment. The expression of those genes in hPASMCs with or without rhPDGF-BB were shown in heatmap (Figure 3D). Next, the enriched pathways of upregulated 49 MAGs were examined by functional annotation tool Metascape. It revealed that pathways including regulation of wound healing, positive regulation of vasculature development, positive regulation of angiogenesis, positive regulation of fibroblast proliferation etc. were enriched in response to rhPDGF-BB treatment as shown in Figure 3E.

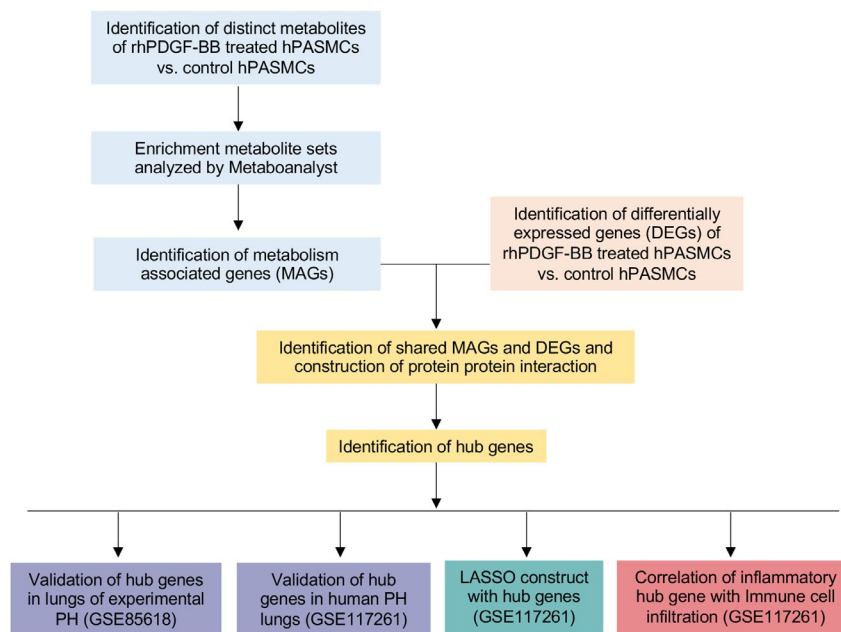


FIGURE 1 Main analysis flowchart. Identification of distinguishing metabolites of recombinant human recombinant PDGF-BB (rhPDGF-BB) treated human pulmonary arterial smooth muscle cells (hPASMCs) versus vehicle treated PASMCs. Enrichment of metabolite sets were analyzed by Metaboanalyst. Top 10 enriched pathways were identified and selected for further identification of metabolism associated genes (MAGs). Next, the shared MAGs and differentially expressed genes (DEGs) in rhPDGF-BB treated hPASMCs versus control cells were identified. Protein protein interaction were constructed. Hub gene were identified by cytoHubba or MCODE add-ins in Cytoscape. Common hub genes were validated in lungs of PH rats after hypoxia exposure from dataset GSE85618 and in lungs of PH patients from dataset GSE117261. LASSO regression model was constructed based on hub genes for PH prediction. The correlation of immune cell infiltration in lung tissues of dataset GSE117261 with inflammatory hub gene was also investigated

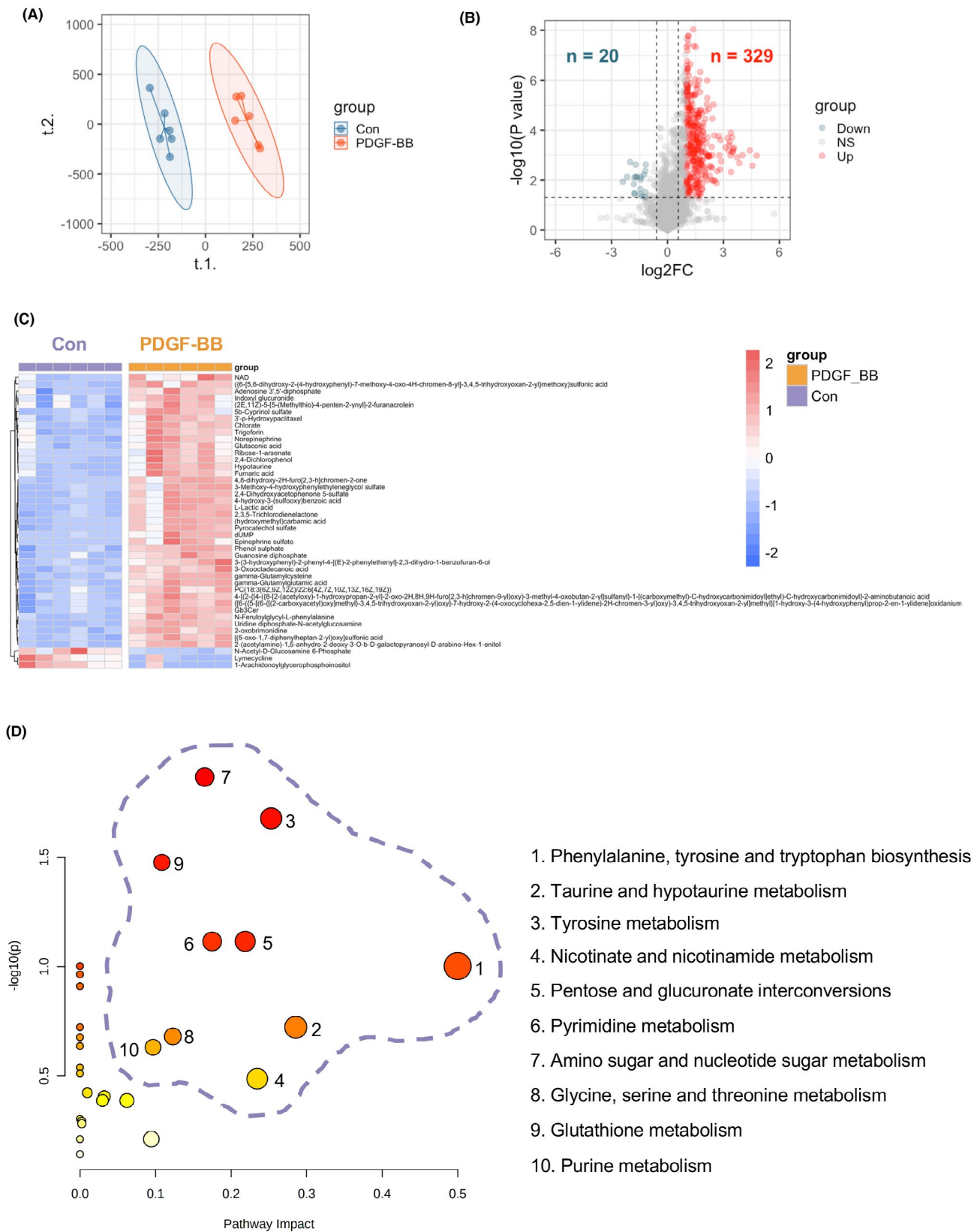


FIGURE 2 Identification of metabolites in response to rhPDGF-BB treatment and enriched pathways of distinguishing metabolites in hPASCs. (A) Partial least squares-discriminant analysis (PLS-DA) demonstrated a well separated sample distribution of rhPDGF-BB treated hPASCs (PDGF-BB) and control hPASCs (Con) and visualized in scatter plot (n = 6). (B) 329 upregulated metabolites (red dots) and 20 down-regulated metabolites (dark green) were identified and visualized in volcano plot (Fold change >2 or <0.5 and p < .05). (C) Expression of distinguishing metabolites including top 40 upregulated and 3 downregulated metabolites with VIP score >1 were visualized in heatmap. (D) Enriched pathways of all distinguishing metabolites (Fold change >2 or <0.5, p < .05 and VIP score >1) were identified in Metaboanalyst

3.3 | Identification of rhPDGF-BB induced proliferation associated hub genes and validation in lungs of human and experimental PH

A total of 152 genes in Figure 3D were then potentially considered as rhPDGF-BB induced proliferation associated MAGs. 411 Protein-protein interactions among the 152 genes were identified and visualized by STRING (Figure S3). Ten hub genes were identified by cytoHubba plugin (Figure 4A) and fourteen hub genes were revealed by MCODE plugin (Figure 4B). In particular, there were nine core hub genes (IL6, CXCL8, CCL2, CXCR4, CCND1, PLAUR, PLAU, HBEGF and F3) identified by both methods. The expressions of nine hub genes were then scrutinized in lungs of PH patients from GSE117261 dataset (Figure 4C). CXCR4 encoding C-X-C motif chemokine receptor

4, CCND1 encoding cyclin D1 and HBEGF encoding heparin binding EGF like growth factor (HB-EGF) were significantly increased in PH patients (all $p < .05$). In addition, Ccl2 encoding C-C motif chemokine ligand 2, Plaur encoding urokinase-type plasminogen activator (u-PA) receptor and Hbegf encoding HB-EGF were elevated in lung tissues of PH rats after hypoxia exposure for 2 weeks compared to that at ambient atmosphere from GSE85618 dataset (Figure 4D).

3.4 | Hub genes-based regression model for PH prediction

In a bid to predict PH, we then sought to construct LASSO regression model based on hub genes. There were 3 genes with

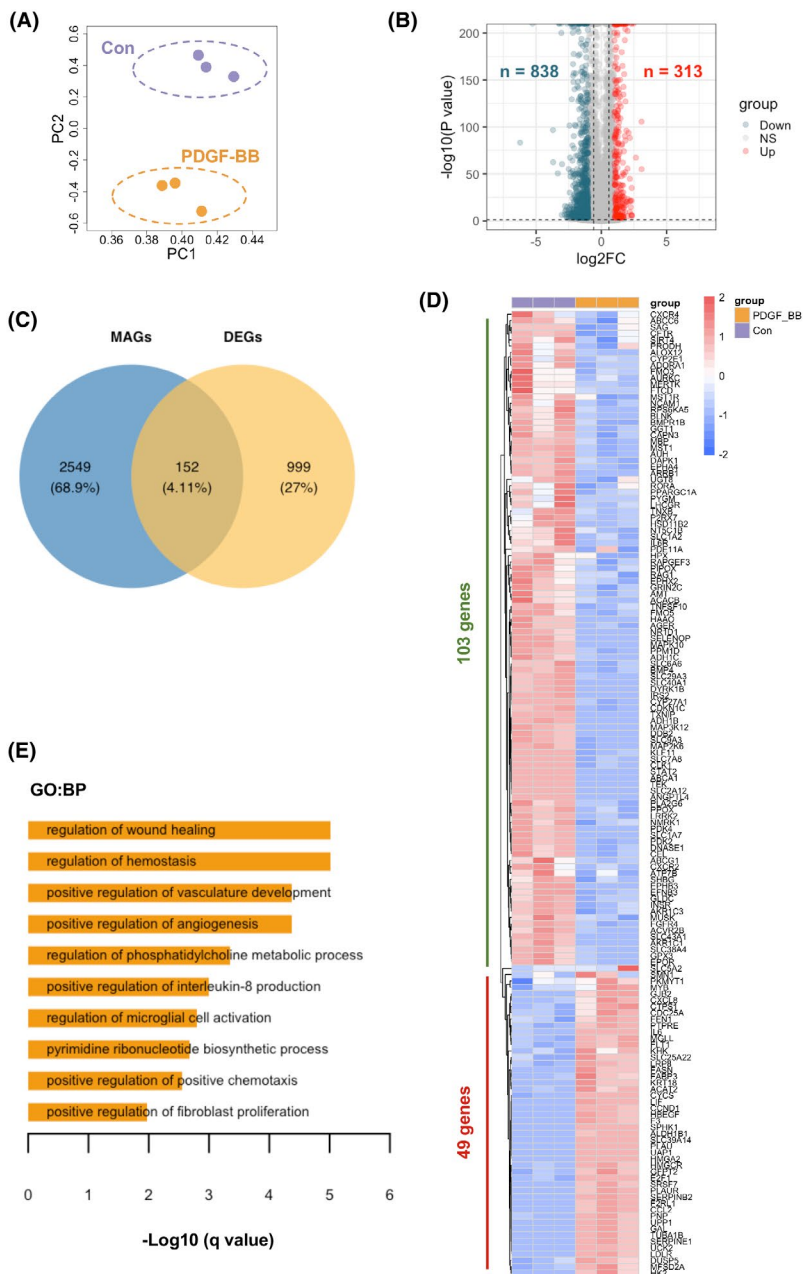


FIGURE 3 Identification of metabolites associated DEGs in response to rhPDGF-BB treatment and enriched pathways in hPASCs. (A) Principal component analysis (PCA) demonstrated a well separated sample distribution of rhPDGF-BB treated hPASCs (PDGF-BB) and control hPASCs (Con) ($n = 3$ per condition). (B) 313 upregulated genes (red dots) and 838 down-regulated metabolites (dark green) were identified and visualized in volcano plot (Fold change >2 or <0.5 and $p < .05$). (C) 152 overlapped metabolites associated genes (MAGs) and DEGs between PDGF-BB group and Con group were visualized in Venn diagram. (D) Expression of 152 overlapped genes (49 upregulated and 103 downregulated genes) were visualized in heatmap in rhPDGF-BB treated hPASCs and control hPASCs. (E) The enriched GO ontology (biological processes) of 49 upregulated genes were identified by functional annotation tool Metascape and visualized in bar plot

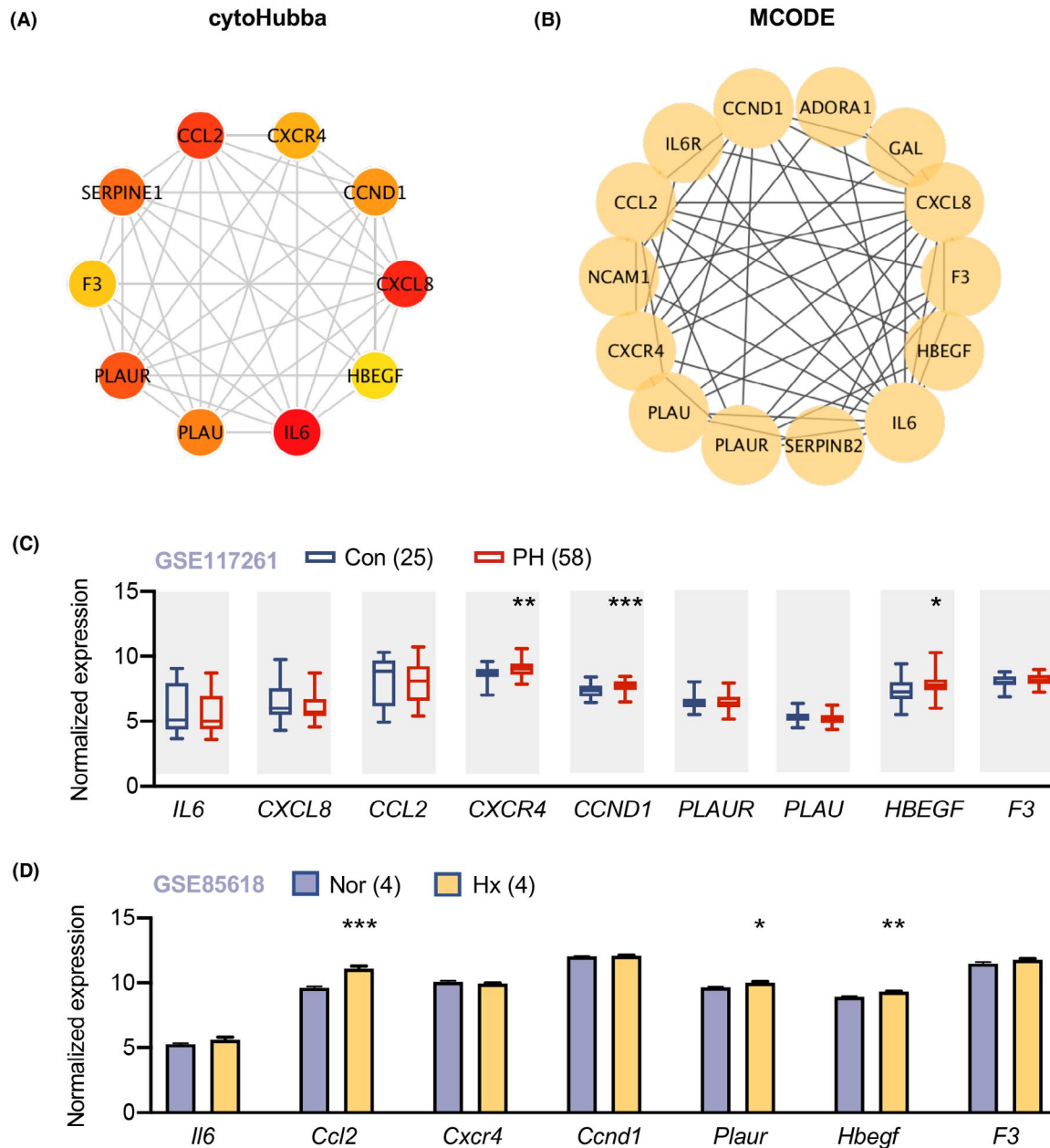


FIGURE 4 Identification of proliferation associated hub genes and validation in lungs of PH patients and PH rat models. (A) Identification of 10 hub genes by cytoHubba in Cytoscape; each circle represents unique gene and the redder the color is, the higher the MCC score is. (B) Identification of 14 hub genes by MCODE in Cytoscape; each circle represents unique gene. (C) Expression of 9 shared hub genes in lungs of 58 patients with pulmonary hypertension (PH) and 25 control subjects from GSE117261 were visualized in box plot. Data represent mean \pm SEM. * $p < .05$, ** $p < .01$, *** $p < .001$ compared to corresponding control subjects, as analyzed by unpaired t test. (D) The expression of hub genes in lungs of rats under hypoxia for two weeks or in normoxic condition ($n = 4$ per group). Data represent mean \pm SEM. * $p < .05$, ** $p < .01$, *** $p < .001$ compared to control rats, as analyzed by unpaired t test

non-zero regression coefficients, and the lambda.min equalled to 0.084. We then generated the hub gene-based model index as follows: $\text{index} = \text{CCND1} * 0.205 + \text{CXCR4} * 0.138 + \text{HBEGF} * (0.022) - 2.253$. According to ROC curve, the area under the curve (AUC) of the model was 0.88 in the training set in Figure 5A and 0.87 in the test set (Figure 5B) from GSE117261 dataset, indicative of a predictor of PH with the established LASSO regression model.

3.5 | The correlation of Immune cell infiltration with CXCR4 expression

As inflammation is considered as a critical trigger of PH development,⁶ we then investigated the association of different inflammatory cell recruitment in human lung tissues with the expression of the inflammation associated hub gene with non-zero regression coefficient (ie. CXCR4), such that we might get a novel insight into

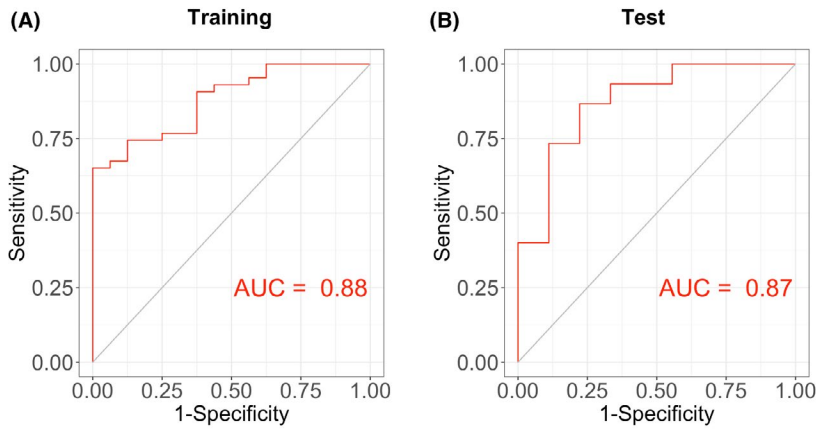


FIGURE 5 Construction of hub gene-based LASSO regression model and its prediction for PH. (A) Receiver operating characteristic (ROC) curve analysis of training set (GSE117261) using nine hub genes. (B) ROC curve analysis of test set (GSE117261) based on nine hub genes. AUC represents area under curve

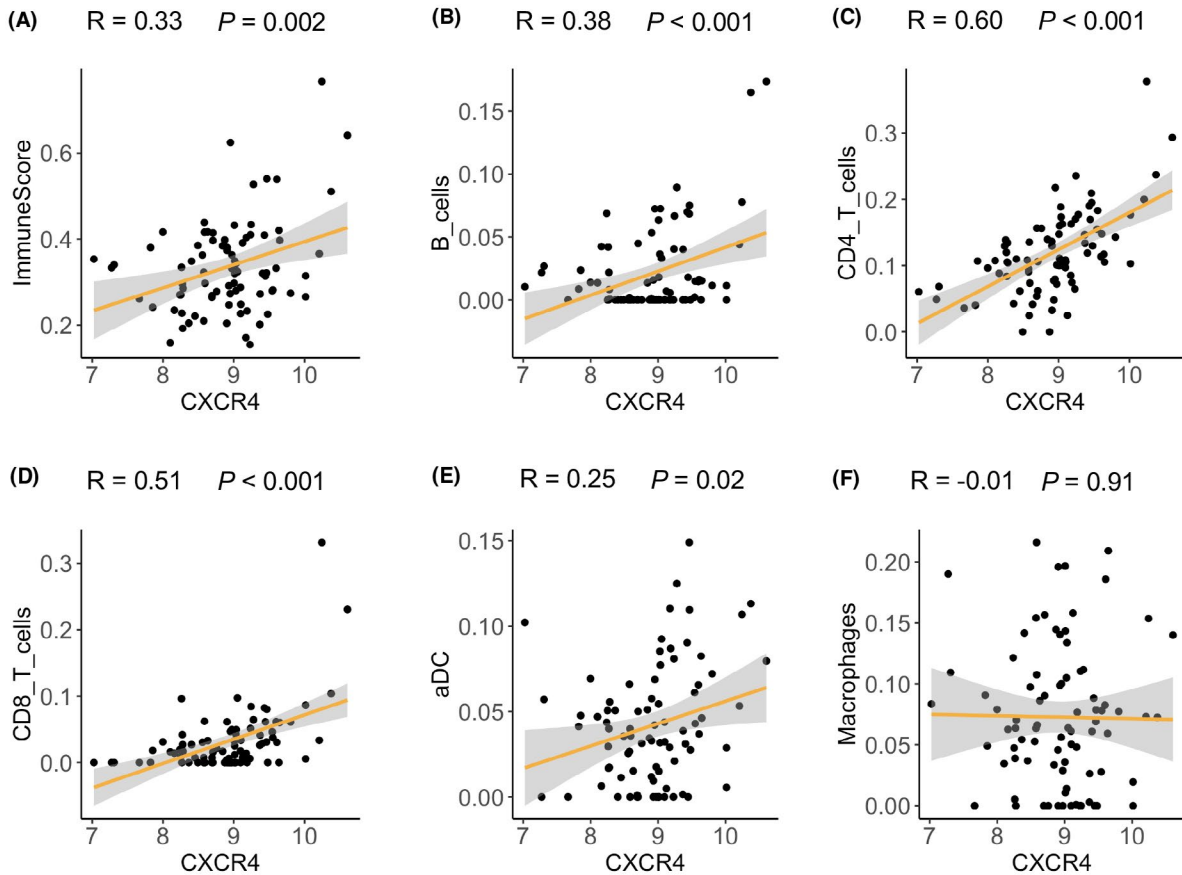


FIGURE 6 Correlation of immune cell infiltration and CXCR4 expression in human lung tissues. (A–F) CXCR4 expression in lung tissues of dataset GSE117261 was positively correlated with (A) ImmuneScore; (B) B cell infiltrates; (C) CD4⁺ T cell infiltrates; (D) CD8⁺ T cell infiltrates; (E) activated dendritic cell infiltrates and (F) macrophage infiltrates

the potential role of CXCR4 in the modulation of specific immune cell type. We found that the expression of CXCR4 was positively correlated to immune cell infiltrates as evidenced by a higher ImmuneScore in human lung tissues with higher CXCR4 levels ($r = .33$, $p = .002$) (Figure 6A). There was also a positive correlation of CXCR4 level with B cells ($r = .38$), CD4⁺ T cells ($r = .60$), CD8⁺ T cells ($r = .51$) and activated dendritic cells ($r = .25$) infiltrates, respectively (all $p < .05$), while no correlation of CXCR4 and macrophages infiltration was observed (Figure 6B–F).

4 | DISCUSSION

In this study, the altered metabolite profiles were revealed by metabolomics and MAGs based on enriched metabolite pathways in hPASCs were identified in response to rhPDGF-BB treatment. In combination of our transcriptomics data, differentially expressed MAGs (ie. main proliferation associated genes) were figured out in rhPDGF-BB treated hPASCs compared to that of control cells, suggesting a crucial link of metabolic adaptations and proliferative

phenotype in hPASCs. We also demonstrated nine hub genes and examined their expressions in lungs of PH patients or hypoxia induced PH rats relative to corresponding controls. Moreover, the hub genes could be predictors for the occurrence of PH, which shed some insight into the development of pulmonary vascular remodeling. In addition, the CXCR4 expression was positively correlated to infiltration of multi-immune cell types in human lung tissues. All these findings implicate a complex metabolic reprogramming and inflammatory modulation in response to proliferation signals, thus mediating the development of PH.

Multi-omics is an emerging strategy that holds promise to discover biomarkers for risk stratification or prognosis and to identify novel therapeutic targets/pathological mechanism in diseased state. For example, metabolomics is now widely used to discover metabolic perturbations or rapid metabolic alteration in response to PH treatment/surgery. It was reported that the plasma metabolic signature of chronic thromboembolic pulmonary hypertension (CTEPH) in pre-pulmonary endarterectomy (PEA) surgery was distinguishing from that of post-PEA surgery.³⁰ Metabolites in response to PEA surgery could serve as suitable noninvasive markers for the evaluation on the therapeutic interventions in the future. In terms of the application of transcriptomics to PH, one of the studies showed that whole blood RNA signature in patients with PAH were distinct from that of control subjects, which was also associated with disease severity and allowed for the identification of patients with poor prognosis.³¹ This study provides important markers for risk stratification and prognosis prediction of PH. In addition, the NIH/NHLBI launched an initiative³² called "Redefining Pulmonary Hypertension through Pulmonary Vascular Disease Phenomics (PVDOMICS)" in 2017, which aims to foster the comprehension in PH based on biological features by virtue of "omics" analysis. This would bring great benefits to the discovery of novel targets and development of more efficacious, precision approaches to individual therapy. In our previous study, we identified spermine as the most dramatically altered metabolite in our PAH cohort by metabolomics and showed that spermine promoted the PASCs proliferation/migration possibly via the modulation of Erk signaling by transcriptomics analysis.⁷ This finding based on multi-omics in our previous study provides the new concept that spermine synthase might be a therapeutic target for PAH. Hence, the combination of transcriptomics and metabolomics of hPASCs in response to the potent mitogen PDGF-BB in the present study would permit the possible discovery of crucial proliferation associated gene markers relevant to the development of PH.

A total of nine proliferation associated hub genes were identified, some of which were cytokine/chemokine related genes. Although the hub gene IL6 didn't differ PH patients or PH rats from their corresponding controls in our selected datasets, lung-specific IL-6 transgenic mice develop spontaneous PH in normoxia and exhibited exaggerated hypoxia-induced PH.³³ In addition, IL-6 blockade mitigated hypoxia-induced PH and repressed the recruitment of Th17 cells and M2 macrophages in lung tissues after hypoxia exposure.³⁴ These findings implicate IL6 as a trigger in pathogenesis of PH. CXCL8 (also named IL8) encoding interleukin-8 was reported to

be higher in serum of PAH patients and had a negative correlation with cardiac index. Kaplan-Meier analysis showed that levels of interleukin-8 predicted survival in PAH patients, with 5-year survival of PAH patients (interleukin-8 levels of >30 pg/ml) to be 32% compared with 58% for patients with levels ≤30 pg/ml.³⁵ Nevertheless, the specific role of CXCL8 in the vasculature homeostasis remains elusive. Another inflammatory hub gene, CCL2, was found to be higher in plasma and lung tissues of IPAH patients in previous study by Sanchez et al.³⁶ although no difference in CCL2 between PH patients and controls were found in dataset GSE117261. The divergency might lie in the heterogeneity of PH cohorts among two studies. In their study, PASCs from PAH patients exhibited stronger migration and proliferation in response to CCL2. This finding suggests a critical role of CCL2 mediated PASC biological activity in vasculature. In Consistent with the higher CXCR4 expression in lungs of PH patients in our study, CXCR4 was also much higher in lungs of PH rat model.³⁷ Of note, SMC specific loss of CXCR4 inhibits SMC proliferation and retards the hypoxia-induced PH.³⁸ This would suggest a detrimental role of CXCR4 in pulmonary vascular remodeling. Intriguingly, CXCR4 expression was positively correlated with B cells-, T cell- (including both CD4⁺ T and CD8⁺ T) and activated dendritic cell infiltration in human lung tissues. However, the mechanism by which CXCR4 mediates various immune cell recruitment into lung tissues in the progression of PH remains poorly understood and warrants further investigation.

For other non-cytokine/chemokine related genes, their roles in maintenance of vascular function have also drawn great attention in PH. There are lines of evidence on the role of CCND1 encoding cyclin D1 in PASCs and pulmonary vascular remodeling, especially in Group 3 PH (PH associated with hypoxia and lung disease). Zeng et al. showed that CCND1 silencing could attenuate the PASC proliferation and cigarette smoke-induced as well as monocrotaline-induced pulmonary vascular remodeling in rats.^{39,40} Moreover, noncoding RNA hsa_circ_0016070 was associated with vascular remodeling in PAH by facilitating the PASCs proliferation via modulation of miR-942/CCND1 axis. The miR-942 level in lung tissues of COPD(+) PH(+) patients (Group 3 PH) was much lower than that in the COPD patients without PH, while the expression of its target genes CCND1 in the Group 3 PH was much higher compared to that of COPD controls.⁴¹ As of today, the PAH targeted therapy against Group 3 PH is not available, the knowledge of the mechanism by which CCND1 mediated PASCs and other vascular cells if possible might offer new opportunity for the treatment of Group 3 PH. PLAU encodes u-PA and PLAUR encodes its receptor u-PA receptor. The deficiency of u-PA dramatically reduced the right ventricular pressure after hypoxia exposure to a comparable level of wild type littermates at normoxic condition, while the loss of u-PA receptor could only partially rescue the increase of right ventricular pressure induced by hypoxia exposure.⁴² According to a recent study by Mirna et al., plasma soluble u-PA receptor was elevated in PH patients and primarily associated with PH due to left sided heart disease.⁴³ However, how u-PA and its receptor orchestrate the vasculature in PH development remains elucidated and is worth further investigation. F3 (also named TF) encodes tissue factor, coagulation

factor III. Previous study showed that higher TF antigen, and TF mRNA in monocytes were displayed in chronic thromboembolic pulmonary hypertension (CTEPH) patients compared with control subjects. TF was also correlated with inflammatory indicators like CRP, TNF- α and CCL2.⁴⁴ Similar to the clinical observation, TF mRNA expression had a positive correlation with media hypertrophy (ratio of vessel wall area to total area) and mean pulmonary arterial pressure in rat model of CTEPH.⁴⁵ The scrutiny of inflammation-coagulation-thrombosis cycle might open new avenue for the treatment of CTEPH. HB-EGF encoded by HBEGF was identified as a mitogen for SMC decades ago and could be induced by multi-mitogens like PDGF.⁴⁶ This is in line with our observation. Besides its role in PSMCs, vascular ECs are able to express HBEGF induced by tumor necrosis factor- α .⁴⁷ These findings would suggest HBEGF may serve as a crucial proliferative signal amplifier and bridge the crosstalk between EC and SMCs in vessels.

Intriguingly, many of the identified hub genes (i.e., IL6, CXCL8, CXCR4, CCND1, PLAUR, PLAU) are hypoxia-inducible factor- α (HIF- α , transcription factor modulating adaptive responses to hypoxia) target genes. HIF-1 α and HIF-2 α are regarded as the main type of HIF- α , an important factor triggering PH development. This implicates a common molecular alteration between PDGF-BB induced and hypoxia induced proliferative phenotype in PSMCs. To support this notion, a previous study showed PDGF promoted the metabolic shift toward glycolysis in PSMCs via activation of the PI3K/AKT/mTOR/HIF-1 α signaling.⁴⁸ This is also in line with another study demonstrating that HIF1 α upregulated genes were enriched in glycolysis and NADH regeneration.⁴⁹ In addition, cytoskeletal protein paxillin tyrosine phosphorylation were elevated in pulmonary vasculature of hypoxia-induced PH mice, which was abolished by

PDGF-BB antagonist (imatinib). In the same study, the increase of paxillin tyrosine phosphorylation in human PSMC was blocked by HIF-1 α depletion or by imatinib, suggesting the augmentation/phosphorylation of paxillin in PSMC responded to PDGF-BB could be at least partially regulated by HIF-1 α .⁵⁰ In addition, HIF-2 α -dependent CXCL12 secretion in PHD2 (prolyl hydroxylase-2)-deficient ECs facilitate PSMCs proliferation and HIF-2 α -selective inhibitor C76 mitigated the established PH rodent models.^{51,52} CXCR4, both HIF- α target gene and identified hub gene in our study, is a well-known chemokine receptor for CXCL12. Therefore, it can be assumed that PHD2-deficient ECs could not only induce PSMCs proliferation, but also foster PSMCs migration and even immune cells accumulation in perivascular spaces in response to CXCL12 release from ECs under hypoxia stress. The modulation of these hub genes would be of great potential for therapeutic benefits in PH as they could impact multiple factors driving PH pathogenesis.

There are some limitations in our study. First, only one dataset of PH lung tissues from human (ie. GSE117261 including 58 PH patients and 25 control subjects) was included. However, the sample size is much larger compared to most of the datasets of human PH lung tissues. Second, the differentially expressed MAGs in hPSMCs in response to PDGF-BB could not fully represent the genes altered in vivo in PH scenario, and their functional properties in pulmonary vascular remodeling need to be investigated in the future.

In conclusion, we identified a metabolic/gene profile change in hPSMCs in response to rhPDGF-BB. The application of multi-omics allows us to discover hub genes to be responsible for proliferating PSMCs phenotype and to be associated with immune cell infiltrates (Figure 7). We consider that improved molecular understanding of

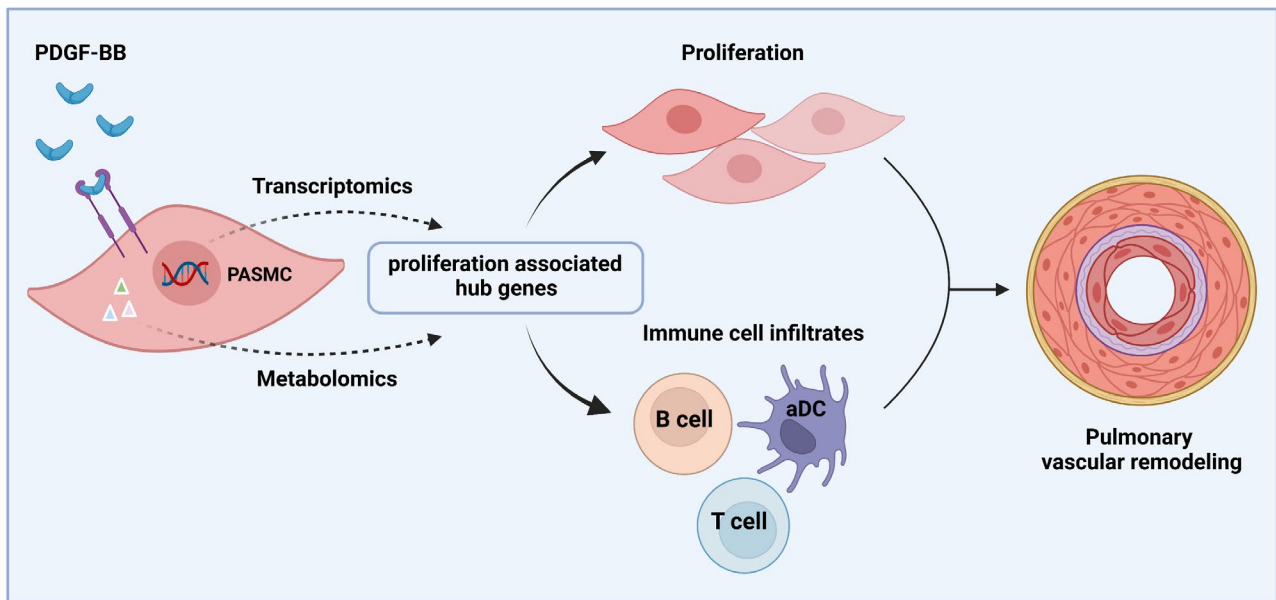


FIGURE 7 Schematic overview. This schematic overview (created with BioRender.com) illustrates that proliferation associated hub genes in PSMCs in response to PDGF-BB were explored by virtue of transcriptomics and metabolomics. Those hub genes were demonstrated to be responsible for proliferating PSMCs phenotype and association with immune cell infiltrates into the lung tissues, contributing to the development of pulmonary vascular remodeling

the intricate networks associated with proliferation in PH will have major therapeutic implications.

ACKNOWLEDGMENTS

None.

CONFLICT OF INTEREST

The authors declare that they have no conflict of interest.

AUTHOR CONTRIBUTIONS

Y. Yan, Y-Y. He and Z-Y. Han designed study design, Y. Yan, R. Jiang and P. Yuan performed data analysis and interpretation, P. Yuan, L. Wen, X-B. Pang and Z-C. Jing provided constructive discussion and revised the manuscript. Z-C. Jing and Y-Y. He provided funding support. Y. Yan, R. Jiang, Y-Y. He and Z-Y. Han wrote the manuscript.

DATA AVAILABILITY STATEMENT

The datasets used in the current study are available from the corresponding authors on reasonable request.

ORCID

Yi Yan  <https://orcid.org/0000-0003-2860-3252>

Ping Yuan  <https://orcid.org/0000-0001-5096-4850>

REFERENCES

- Hoeper MM, Bogaard HJ, Condliffe R, et al. Definitions and diagnosis of pulmonary hypertension. *J Am Coll Cardiol*. 2013;62:D42-D50.
- International PPHC, Lane KB, Machado RD, Pauculo MW, et al. Heterozygous germline mutations in BMPR2, encoding a TGF-beta receptor, cause familial primary pulmonary hypertension. *Nat Genet*. 2000;26:81-84.
- Southgate L, Machado RD, Graf S, Morrell NW. Molecular genetic framework underlying pulmonary arterial hypertension. *Nat Rev Cardiol*. 2020;17:85-95.
- Liu D, Yan Y, Chen JW, et al. Hypermethylation of BMPR2 promoter occurs in patients with heritable pulmonary arterial hypertension and inhibits BMPR2 expression. *Am J Respir Crit Care Med*. 2017;196:925-928.
- Yan Y, He YY, Jiang X, et al. DNA methyltransferase 3B deficiency unveils a new pathological mechanism of pulmonary hypertension. *Sci Adv*. 2020;6:eaba2470.
- Rabinovitch M, Guignabert C, Humbert M, Nicolls MR. Inflammation and immunity in the pathogenesis of pulmonary arterial hypertension. *Circ Res*. 2014;115:165-175.
- He YY, Yan Y, Jiang X, et al. Spermine promotes pulmonary vascular remodelling and its synthase is a therapeutic target for pulmonary arterial hypertension. *Eur Respir J*. 2020;56:2000522.
- Zhao JH, He YY, Guo SS, et al. Circulating plasma metabolomic profiles differentiate rodent models of pulmonary hypertension and idiopathic pulmonary arterial hypertension patients. *Am J Hypertens*. 2019;32:1109-1117.
- Naeije R, Dedobbeleer C. Pulmonary hypertension and the right ventricle in hypoxia. *Exp Physiol*. 2013;98:1247-1256.
- de Jesus Perez VA. Molecular pathogenesis and current pathology of pulmonary hypertension. *Heart Fail Rev*. 2016;21:239-257.
- Galiè N, Humbert M, Vachiery JL. 2015 ESC/ERS guidelines for the diagnosis and treatment of pulmonary hypertension: the joint task force for the diagnosis and treatment of pulmonary hypertension of the European Society of Cardiology (ESC) and the European Respiratory Society (ERS): endorsed by: Association for European Paediatric and Congenital Cardiology (AEPCC), International Society for Heart and Lung Transplantation (ISHLT). *Eur Heart J*. 2016;37(1):67-119.
- Lau EMT, Giannoulatou E, Celermajer DS, Humbert M. Epidemiology and treatment of pulmonary arterial hypertension. *Nat Rev Cardiol*. 2017;14:603-614.
- Spiekerkoetter E, Tian X, Cai J, et al. FK506 activates BMPR2, rescues endothelial dysfunction, and reverses pulmonary hypertension. *J Clin Invest*. 2013;123:3600-3613.
- Liu D, Wu BX, Sun N, et al. Elevated levels of circulating bone morphogenetic protein 7 predict mortality in pulmonary arterial hypertension. *Chest*. 2016;150:367-373.
- Atkinson C, Stewart S, Upton PD, et al. Primary pulmonary hypertension is associated with reduced pulmonary vascular expression of type II bone morphogenetic protein receptor. *Circulation*. 2002;105:1672-1678.
- Chen PH, Chen X, He X. Platelet-derived growth factors and their receptors: structural and functional perspectives. *Biochim Biophys Acta*. 2013;1834:2176-2186.
- Perros F, Montani D, Dorfmüller P, et al. Platelet-derived growth factor expression and function in idiopathic pulmonary arterial hypertension. *Am J Respir Crit Care Med*. 2008;178:81-88.
- Griminger F, Schermuly RT. PDGF receptor and its antagonists: role in treatment of PAH. *Adv Exp Med Biol*. 2010;661:435-446.
- Schermuly RT, Dony E, Ghofrani HA, et al. Reversal of experimental pulmonary hypertension by PDGF inhibition. *J Clin Invest*. 2005;115:2811-2821.
- Hu Y, Chi L, Kuebler WM, Goldenberg NM. Perivascular inflammation in pulmonary arterial hypertension. *Cells*. 2020;9:2338.
- Yan Y, Wang XJ, Li SQ, et al. Elevated levels of plasma transforming growth factor-beta1 in idiopathic and heritable pulmonary arterial hypertension. *Int J Cardiol*. 2016;222:368-374.
- Chong J, Wishart DS, Xia J. Using MetaboAnalyst 4.0 for comprehensive and integrative metabolomics data analysis. *Curr Protoc Bioinformatics*. 2019;68:e86.
- Safran M, Dalah I, Alexander J, et al. GeneCards Version 3: the human gene integrator. *Database (Oxford)*. 2010;2010:baq020.
- Zhou Y, Zhou B, Pache L, et al. Metascape provides a biologist-oriented resource for the analysis of systems-level datasets. *Nat Commun*. 2019;10:1523.
- Szklarczyk D, Gable AL, Lyon D, et al. STRING v11: protein-protein association networks with increased coverage, supporting functional discovery in genome-wide experimental datasets. *Nucleic Acids Res*. 2019;47:D607-D613.
- Shannon P, Markiel A, Ozier O, et al. Cytoscape: a software environment for integrated models of biomolecular interaction networks. *Genome Res*. 2003;13:2498-2504.
- Stearman RS, Bui QM, Speyer G, et al. Systems analysis of the human pulmonary arterial hypertension lung transcriptome. *Am J Respir Cell Mol Biol*. 2019;60:637-649.
- Frump AL, Albrecht ME, McClintick JN, Lahm T. Estrogen receptor-dependent attenuation of hypoxia-induced changes in the lung genome of pulmonary hypertension rats. *Pulm Circ*. 2017;7:232-243.
- Aran D, Hu Z, Butte AJ. xCell: digitally portraying the tissue cellular heterogeneity landscape. *Genome Biol*. 2017;18:220.
- Swietlik EM, Ghataorhe P, Zaleska KI, et al. Plasma metabolomics exhibit response to therapy in chronic thromboembolic pulmonary hypertension. *Eur Respir J*. 2021;57:2003201.
- Rhodes CJ, Otero-Nunez P, Wharton J, et al. Whole-Blood RNA profiles associated with pulmonary arterial hypertension and clinical outcome. *Am J Respir Crit Care Med*. 2020;202:586-594.
- Hemnes AR, Beck GJ, Newman JH, et al.; Group PS. PVDOMICS: a multi-center study to improve understanding of pulmonary vascular disease through phenomics. *Circ Res*. 2017;121:1136-1139.

33. Steiner MK, Syrkinina OL, Kolliputi N, Mark EJ, Hales CA, Waxman AB. Interleukin-6 overexpression induces pulmonary hypertension. *Circ Res*. 2009;104:236-244. 28p following 244.
34. Hashimoto-Kataoka T, Hosen N, Sonobe T, et al. Interleukin-6/interleukin-21 signaling axis is critical in the pathogenesis of pulmonary arterial hypertension. *Proc Natl Acad Sci USA*. 2015;112:E2677-E2686.
35. Soon E, Holmes AM, Treacy CM, et al. Elevated levels of inflammatory cytokines predict survival in idiopathic and familial pulmonary arterial hypertension. *Circulation*. 2010;122:920-927.
36. Sanchez O, Marcos E, Perros F, et al. Role of endothelium-derived CC chemokine ligand 2 in idiopathic pulmonary arterial hypertension. *Am J Respir Crit Care Med*. 2007;176:1041-1047.
37. Zhang T, Kawaguchi N, Hayama E, Furutani Y, Nakanishi T. High expression of CXCR4 and stem cell markers in a monocrotaline and chronic hypoxia-induced rat model of pulmonary arterial hypertension. *Exp Ther Med*. 2018;15:4615-4622.
38. Dai Z, Zhu MM, Peng Y, et al. Endothelial and smooth muscle cell interaction via FoxM1 signaling mediates vascular remodeling and pulmonary hypertension. *Am J Respir Crit Care Med*. 2018;198:788-802.
39. Zeng DX, Xu GP, Lei W, Wang R, Wang CG, Huang JA. Suppression of cyclin D1 by plasmid-based short hairpin RNA ameliorated experimental pulmonary vascular remodeling. *Microvasc Res*. 2013;90:144-149.
40. Zeng DX, Liu XS, Xu YJ, et al. Plasmid-based short hairpin RNA against cyclin D1 attenuated pulmonary vascular remodeling in smoking rats. *Microvasc Res*. 2010;80:116-122.
41. Zhou S, Jiang H, Li M, et al. Circular RNA hsa_circ_0016070 is associated with pulmonary arterial hypertension by promoting PSMC proliferation. *Mol Ther Nucleic Acids*. 2019;18:275-284.
42. Levi M, Moons L, Bouche A, Shapiro SD, Collen D, Carmeliet P. Deficiency of urokinase-type plasminogen activator-mediated plasmin generation impairs vascular remodeling during hypoxia-induced pulmonary hypertension in mice. *Circulation*. 2001;103:2014-2020.
43. Mirna M, Rohm I, Jirak P, et al. Analysis of novel cardiovascular biomarkers in patients with pulmonary hypertension (PH). *Heart Lung Circ*. 2020;29:337-344.
44. Yang M, Deng C, Wu D, et al. The role of mononuclear cell tissue factor and inflammatory cytokines in patients with chronic thromboembolic pulmonary hypertension. *J Thromb Thrombolysis*. 2016;42:38-45.
45. Deng C, Wu D, Yang M, et al. Expression of tissue factor and forkhead box transcription factor O-1 in a rat model for chronic thromboembolic pulmonary hypertension. *J Thromb Thrombolysis*. 2016;42:520-528.
46. Dluz SM, Higashiyama S, Damm D, Abraham JA, Klagsbrun M. Heparin-binding epidermal growth factor-like growth factor expression in cultured fetal human vascular smooth muscle cells. Induction of mRNA levels and secretion of active mitogen. *J Biol Chem*. 1993;268:18330-18334.
47. Yoshizumi M, Kourembanas S, Temizer DH, Cambria RP, Quertermous T, Lee ME. Tumor necrosis factor increases transcription of the heparin-binding epidermal growth factor-like growth factor gene in vascular endothelial cells. *J Biol Chem*. 1992;267:9467-9469.
48. Xiao Y, Peng H, Hong C, et al. PDGF promotes the Warburg effect in pulmonary arterial smooth muscle cells via activation of the PI3K/AKT/mTOR/HIF-1alpha signaling pathway. *Cell Physiol Biochem*. 2017;42:1603-1613.
49. Downes NL, Laham-Karam N, Kaikkonen MU, Yla-Herttua S. Differential but complementary HIF1alpha and HIF2alpha transcriptional regulation. *Mol Ther*. 2018;26:1735-1745.
50. Veith C, Zakrzewicz D, Dahal BK, et al. Hypoxia- or PDGF-BB-dependent paxillin tyrosine phosphorylation in pulmonary hypertension is reversed by HIF-1alpha depletion or imatinib treatment. *Thromb Haemost*. 2014;112:1288-1303.
51. Dai Z, Li M, Wharton J, Zhu MM, Zhao YY. Prolyl-4 hydroxylase 2 (PHD2) deficiency in endothelial cells and hematopoietic cells induces obliterative vascular remodeling and severe pulmonary arterial hypertension in mice and humans through hypoxia-inducible factor-2alpha. *Circulation*. 2016;133:2447-2458.
52. Dai Z, Zhu MM, Peng Y, et al. Therapeutic targeting of vascular remodeling and right heart failure in pulmonary arterial hypertension with a HIF-2alpha inhibitor. *Am J Respir Crit Care Med*. 2018;198:1423-1434.

SUPPORTING INFORMATION

Additional supporting information may be found in the online version of the article at the publisher's website.

How to cite this article: Yan Y, Jiang R, Yuan P, et al. Implication of proliferation gene biomarkers in pulmonary hypertension. *Anim Models Exp Med*. 2021;4:369-380. doi:[10.1002/ame2.12191](https://doi.org/10.1002/ame2.12191)